

CHAPTER - 3

GEOLOGICAL SETTING

3.1 Introduction

The Indian subcontinent is divided into two Archean cratonic blocks by the Central Indian Tectonic Zone (CITZ), which runs in the ENE–WSW direction; the northern and southern cratonic blocks (Basu, 1986). The southern Indian block includes Bastar, Dharwar, and Singhbhum cratons, while the northern Indian block includes the cratons of Bundelkhand and Aravalli. According to Naqvi and Rogers (1987), the Great Boundary Fault is the main boundary that divides the northern Indian block into two blocks. The eastern block is known as the Aravalli cratonic block, and the western block is known as the Bundelkhand cratonic block. The Bundelkhand Craton (BuC) is of semi-circular shape, having an area of about 45,000 km² of which only 26,000 km² is exposed as an outcrop between 24°11' to 26°27'N and 78°10' to 81°24'E and the rest is covered by alluvium of the Ganga basin (Fig.3.1). Among the many Archean cratons of India, BuC has perhaps the most complex evolutionary history (Gokarn et al., 2013). It has been broadly agreed that many micro-blocks are united to form the basement of the BuC, which is of the Archean age (Mohan et al. 2012). In the west, the BuC is fringed by the Great Boundary Fault (GBF), trending NE–SW, in the north-west by the Gwalior Basin, in the south by the Sonarai Basin, and by the Bijawar marginal basins in the south-east (Basu, 1986; Mondal et al. 2002). The Vindhyan Supergroup overlies the marginal basins and surrounds the BuC on three sides. The Gangetic alluvial plains cover the craton on the northern side (Basu, 1986), but the southwestern part is hidden beneath the Deccan basalts (Pandey et al., 2011).

3.2 Geology and stratigraphy of the Bundelkhand craton

BuC comprises Bundelkhand gneissic complex (BnGC), Bundelkhand metavolcanic and metasediments (BMM), Madawara igneous complex (MIC), Bundelkhand granitoids

(BG) of different episodes, Quartz reef (QR), Mafic dyke swarms (MDS), Banded Iron Formations (BIFs) (Pradhan et al. 2012, Kumar et al. 2013, Pandey et al. 2011) (Table 1). A thick shear zone designated as Bundelkhand tectonic zone (BTZ) cuts across the BuC, striking approximately E-W and consisting of pillow basalts, gneisses and metasediments (Gokharan et al. 2013). According to Malviya et al. (2006), pillow basalts are thought to have formed due to volcanic activity in the BTZ region in a subduction zone. BTZ divides the Bundelkhand craton into two parts, commonly known as Central and Southern Bundelkhand Craton, based on deformation and metamorphic events and the nature of rocks exposed there, such as greenstone belts, layered mafic-ultramafic intrusions, BIFs (Verma et al., 2016; Joshi et al., 2017; Singh et al., 2019).

The BuC is divided into two large E-W trending greenstone belts, the northern belt and the southern belt, which contain supracrustal units tectonically embedded with TTGs. The northern belt, also known as the Central Bundelkhand Greenstone belt (CBGB), runs through Mauranipur, Kuraicha, and is exposed in the middle of BuC. This belt stretches from Babina in the west to Mahoba in the east and is well exposed in the Babina and Mauranipur areas containing metamorphosed basic rocks of Paleo-Mesoarchean age (Malviya et al. 2006; Singh et al. 2019), felsic volcanic rocks of Mesoarchean age (Slabunov & Singh 2019), and metasedimentary rocks (BIFs). Pink granites and granodiorites (2.58–2.51 Ga) cut this belt at different orientations, showing an intrusive relationship with the rocks of CBGB and being undeformed (Joshi et al., 2013; Kaur et al., 2016). CBGB shows an angular relationship with BnGC, which is older (3.5–3.2 Ga) (Singh et al., 2018; Kaur et al., 2014; Saha et al., 2016). Sinistral movement of rocks in the greenstone belt by quartz reefs is also reported (Singh et al., 2019). The Babina and Bhauti areas in the CBGB contain felsic volcanic rocks of 2.5–2.6 Ga (Pandey et al., 2011, Singh and Slabunov, 2016). According to existing geochronological data, ultramafic-mafic magmatism marks the beginning of the CBGB around 2.78 Ga, and

felsic volcanism marks the termination of the CBGB around 2.54 Ga (Singh et al., 2019). The southern belt stretches from Madaura to Girar and contains a sequence of ultramafic-mafic volcanic rocks, quartzite, BIF, chlorite schist, and marble (Singh and Slabunov, 2015; Nasipuri et al., 2019). The description of different rock types exposed along these two belts and in the BuC is given below and summarised in Table 3.1.

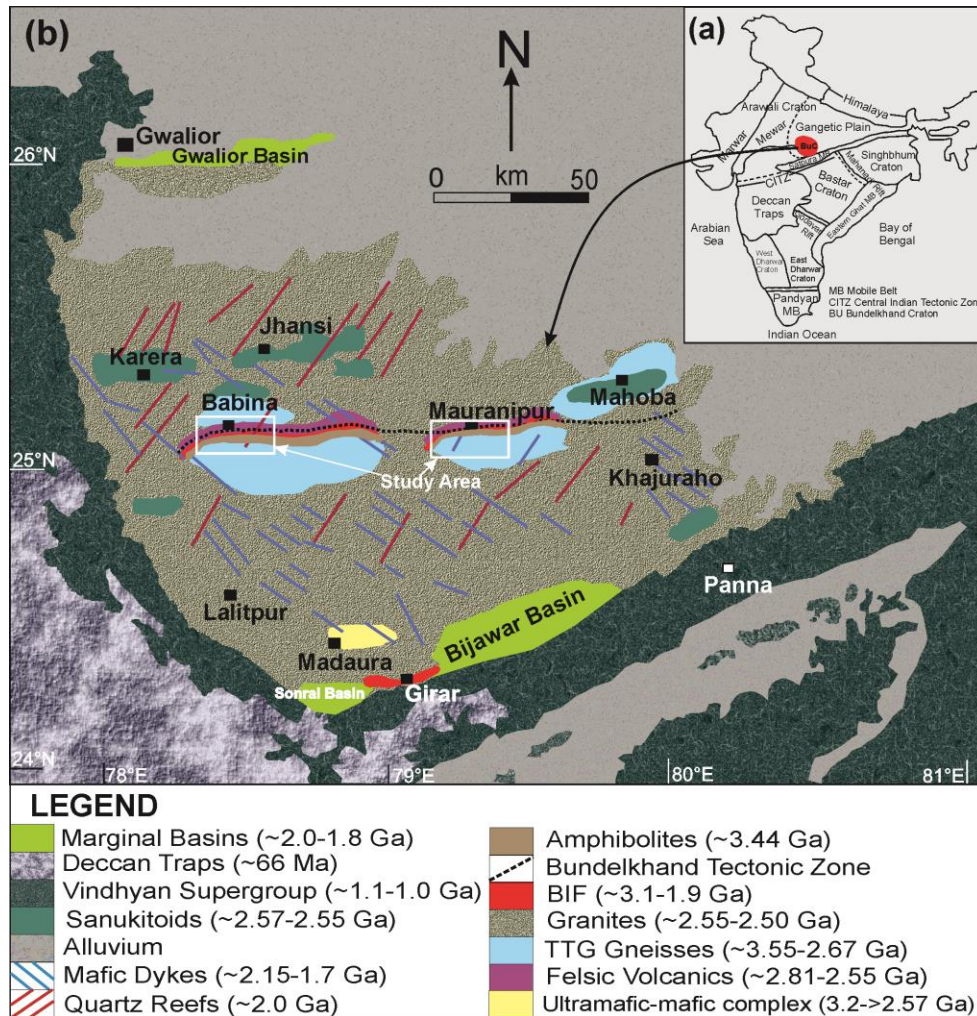


Figure 3.1 (a) Inset map showing the location of Bundelkhand Craton in Indian shield (after Singh & Dwivedi, 2015). (b) Geological map of Bundelkhand Craton with its location in India (after Singh et al. 2021).

3.2.1. Tonalite-Trondhjemite-Granodiorite Gneisses (TTGs)

The TTGs form an important Archean crustal component throughout the world. The TTGs of the Bundelkhand massif are of different ages, ranging from 3.6–2.7 Ga, and mainly occur as relict components, as patches within alkaligranitoid gneisses of the Archean

age (Basu 1986; Joshi et al., 2017). They are also reported from the southern part of the BuC (Prakash et al., 1975). The TTGs are comprised mainly of plagioclase feldspar, quartz, biotite, calcic-amphibole, and K-feldspar, having epidote, zircon, monazite, apatite, and titanite as accessory phases (Chauhan et al., 2018). Bundelkhand gneisses show polyphase deformation with well-developed foliations and are strongly dipping towards 50°N. They are mainly sodic to potassic in composition, having low HREE character with a low Eu anomaly (Joshi et al., 2017). It has been suggested that the BnGC is the oldest component of the BuC (; Mondal et al., 2002).

3.2.2. Metasupracrustals associated with greenstone belts

Singh & Slabunov (2015) reported two supracrustal greenstone belts in the BuC. The Central Bundelkhand Greenstone Belt (CBGB) (Babina and Mauranipur) is the first, and the Southern Bundelkhand Greenstone Belt (SBGB) is the second (Girar, Madaura belt) (Singh et al. 2019). The geological units exposed in the CBGB are felsic volcanic rocks, mafic-ultramafic rocks, and BIFs (Malviya et al., 2006). In contrast, the SBGB primarily comprises quartzite, sericite schist, and BIFs (Slabunov et al., 2017). The central portion of the craton has an E-W trending exposure of granite-greenstone rocks for 200 km. This exposure runs parallel to the Bundelkhand Tectonic Zone, which connects Mahoba to Babina via Mauranipur (Malviya et al., 2006; Pati et al., 2007). The CBGB is further subdivided into two greenstone belts, the Mauranipur and Babina greenstone belts, both of which trend east-west and are exposed in a straight belt (Singh & Slabunov, 2015a,b). Both greenstone belts are medium to low-grade metamorphosed and contain ultramafic/mafic-felsic volcanic and metasedimentary geological units (BIFs) of the Paleoproterozoic age (Malviya et al. 2006). The supracrustal rocks have intruded into the basement unit and display sheared/faulted contact with TTGs. The granite and granodiorite are of 2.5 Ga age and intrude the greenstone sequence (Kaur et al., 2016; Joshi et al., 2017), while the Mesoproterozoic Bundelkhand gneiss

associated with the Archean greenstone belt is dated between 3.5 and 3.2 Ga (Saha et al., 2016; Nasipuri et al., 2019).

3.2.3. Amphibolites

Amphibolites are unveiled mainly in the CBGC and the Bundelkhand tectonic zone (Pati 2020). But they are also present as enclaves within gneisses and granitoids. Here, various rock types such as BIF, white schists, calc-silicate rocks, quartzites, and metapelites are also exposed, along with amphibolites. Two types of amphibolites are found here; one is garnet-free amphibolites, and the other one is garnet-containing amphibolites. Both display a nematogranoblastic texture in which all the previous textures and structures are wiped out (Singh and Slabnouv 2015). Amphibolites are mainly exposed as lenticular patches and bands within pelitic gneisses. Mineralogically amphibolites contain hornblende + plagioclase ± garnet ± biotite ± chlorite ± quartz ± magnetite ± sphene ± apatite ± zircon ± monazite etc. (Pati and Saha, 2011). The Nd isotopic values of amphibolites provide two model ages, one for the protolith of the amphibolites as 4.9–4.2 Ga and the second for the metamorphism of amphibolites as 3.4–3.3 Ga (Malviya et al., 2006; Singh et al., 2019; Pati 2020). The Nd values suggest that the amphibolites are formed in a subduction-related environment.

3.2.4. Pillow basalts

The pillow basalts are mostly exposed along the Pal, Basti, and Bargaon areas of Mauranipur. They are mainly amalgamated with BIFs and metamorphosed ultramafic rocks (Malviya et al., 2006). In the vicinity of BTZ, quartz veins and mylonitized granitoids are associated with pillow basalts and cross-cutting them. They are mineralogically composed of hornblende, plagioclase, magnetite, epidote, chlorite, and quartz. Pillow basalts are mainly archean age (Sarkar et al., 1994; Mondal et al., 2002). The average length of pillow basalts is 50 cm, with an aspect ratio between 3.0 and 4.5. The pillow basalts are believed to have been generated by an island arc tectonic setting (Malviya et al., 2006).

3.2.5. Banded iron formations (BIFs)

The BuC contains BIF bands of Mesoarchean age trending E-W and is best exposed in the CBGB. The BIF bands steeply dipped towards the north, up to 65° and displayed three phases of folding (Basu 1986). The BIF bands are exposed in Babina, Prithvipura, Sukwan-Dukwan, Papaoni, Gora, Balyara, Kuraicha, Mauranipur, Santhar, and Bijainagar-Thanasagar-Paswara (Mahoba) and have tectonic association with basic-ultrabasic, felsic volcanic, amphibolites, quartzites, pillow basalts, and calc-silicate rocks. The BIFs of the south Bundelkhand craton are of Neoproterozoic age and are in contact with quartzite and dolomites (Singh et al., 2018). Magnetite and quartz layers alternately are exposed in banded iron formations (BIFs) in BuC, similar to other Indian cratons and different parts of the world. The banded iron formations have suffered greenschist to upper amphibolite/granulite facies metamorphism (Pati, 1999). The iron formations mainly include banded quartz-magnetite rock, banded magnetite amphibolite rock, and banded amphibolites. The common silicates and oxides noted in BIFs include magnetite, quartz, orthopyroxene, clinopyroxene, garnet, hornblende, actinolite, biotite, chlorite, apatite, and ± allanite. The BIF has three distinct mineral assemblages (1. Mag + Amp + Chl + Ap + Qtz; 2. Mag + Grt + Opx + Cpx + Ap + Qtz; and 3. Mag + Amp + Chl + Grt + Ap + Qtz).

3.2.6 Madawara Ultramafic Complex (MUC)

Located at the southern boundary of the BuC, the MUC has been identified as a possible source of platinum group elements (PGEs) in north-central India (Pati et al., 2007; Farooqui and Singh, 2006; Singh et al., 2018). MUC is a grouping of variously altered and metamorphosed (deformed) mafic and ultramafic rocks (metadunite, metaperidotite (hornblende), metapyroxenite (olivine), gabbro, and diorite) that occur as E-W-trending lensoidal bodies over an area of about 400 sq km (Mohanty et al., 2018; Ramiz et al., 2018). Integration of field, petrography and bulk rock geochemistry have been carried out in MUC

to understand its petrogenesis and tectonic evolution (Mohanty et al., 2018; Ramiz et al., 2018). The most prominent ultramafic outcrop exposed in the southeast of Madawara Village is a 400 m thick, low-lying ridge (Mohanty et al., 2018). The rocks of this complex are mainly constricted between the Madawara Shear in the north and the Sonrai-Girar Shear in the south and have undergone greenschist to lower amphibolite facies metamorphism (Satyanarayanan et al., 2015; Ramiz et al., 2018). The whole sequence of mafic-ultramafic rocks of this complex is cut across by dolerite dykes (Singh et al., 2018). Generally, the contacts between ultramafic rocks and Bundelkhand granite-gneisses are sheared and mylonitized in the area (Singh et al., 2018; Ramiz et al., 2018). Recent geochemical studies have revealed that rocks in this region are enriched in light rare earth elements (LREEs), and LILEs compared to HREEs and HFSEs, indicating that the MUC is located in a continental arc (Mohanty et al., 2018; Ramiz et al., 2018).

3.2.7 Intrusive Granitoids, Syenites and Pegmatites

The granitic magmatism in BuC occurred between 1.9 and 2.58 Ga (Joshi et al., 2017; Singh et al., 2019). Based on colour, mineral composition, texture, and location, the Bundelkhand granitoids are classified into different categories as leuco-, pink, and grey granites; aplite, medium and coarse-grained granites; porphyritic, rapakivi, and orbicular granites; foliated biotite granite, porphyritic biotite granite, coarse grain leucogranite, fine-grained granite, and hornblende granite; monzogranite, syenogranite, and granodiorite, Jhansi, Matatila, and Garhmau granites (Singh et al., 2021). The main granitic types form large batholithic bodies. They have mainly calc-alkaline, metaluminous to peraluminous chemistry, representing a volcanic arc affinity, and have a significant variation in SiO₂ concentration (Mondal and Zainuddin, 1996; Ray et al., 2015). These rocks have high Rb, intermediate Nb, and Nd values, and they are mostly I- to A-type granites that formed during syn- to post-collision events. The granitoids have a poorly fractionated chondrite normalized

rare earth element distribution pattern, as well as a negative Europium (Eu) anomaly, indicating subduction. Granodiorite-granite series rocks originate mostly in volcanic arc settings, whereas potash-rich granites form in syn-collisional to post-collisional settings. On the basis of geochemical attributes it is deduced that the granitoids are formed in a subduction environment by partially melting the Paleo- Mesoarchean TTGs or mafic (Ray et al., 2015; Singh et al., 2019). Based on their geochemical diversity, Joshi et al. (2017) classified them as Low-Silica High-Magnesium (LSHM) granitoids (e.g. sanukitoids and Closepet type granitoids) and High-Silica Low-Magnesium (HSLM) granitoids (e.g. monzogranites). Also, Joshi et al. (2017) recognized the existence of sanukitoids in BuC for the first time and discussed their tectonic setting. These sanukitoids were intruded by high-K granite at several places. In general, the mineralogy of these sanukitoids includes plagioclase, hornblende, biotite, and quartz. In contrast, quartz and K-feldspar are common minerals in high-K anatectic granites with plagioclase, biotite, zircon, apatite, monazite, titanite, and allanite occurring as accessories (Singh et al., 2019). According to Joshi et al. (2017) and Singh et al. (2019), the geochemistry of sanukitoids shows high SiO₂, Mg#, Cr, and Ni with a relatively higher concentration of K₂O, Ba, Sr, and ferromagnesian oxides.

3.2.8 Giant Quartz Veins (GQVs)

The quartz veins are exposed as ridges trending NE-SW in the BuC. They rise to 100–175 m, like walls and ridges, and extend to 60 km. Eleven major quartz reefs are reported from BuC. The longest is the Newari quartz reef, which is traceable for 100 km in length. Fault breccias, intense mylonitization, and subhorizontal stretching lineations are exposed along the narrow zones of quartz reefs. The quartz reefs mainly show pinkish white, greyish white, and milky white. The mineralogy of quartz reefs includes mostly quartz (84 and 96 wt.%) with <5 modal% of ± sericite, ± epidote, ± opaques and ± calcite (Pati et al., 2007). The K-Ar chronological data suggests the GQVs' formation between 1.9 and 2.0 Ga (Pati et al.,

1997; Pati et al., 2007). The emplacement of quartz reefs along the brittle-ductile shear zones marked the end stage of craton formation. It represents hydrothermal activity after the crystallization of granitic plutons.

3.2.9 Mafic Dykes

NW-SE trending mafic dykes of olivine tholeiite to quartz tholeiite composition are characteristic of the BuC. They are exposed for over 50 km, cutting across the NE-SW trending quartz reefs. They show low relief, unlike quartz reefs. They are emplaced within granitoids having sharp contacts showing chilled margins. Some mafic dykes occasionally show an N-S to ENE-WSW trend (Pati et al., 2007). Most dykes are traceable for long distances and discontinuous like linear ridges and show echelon fractures and joints. The dykes are dark greenish grey, showing three generations of origins as coarse-grained variety, medium-grained variety, and fine-grained with ophitic to sub-ophitic texture. Primary igneous textures are well preserved. The mineralogy includes plagioclase (dominant mineral 45-50%), clinopyroxene (Cpx, 30-45 %), orthopyroxene (Opx, <1 to 2 %), quartz (Qtz, <1 to 2 %), magnetite (Mag) and titanomagnetite (1-4 %) and olivine (Ol, <1 %). In addition, \pm ilmenite (Il), \pm apatite (Ap), \pm alkali feldspar and \pm glass (Gl; devitrified) occur in the mode.

3.3 Geology around Mauranipur and Babina region

The study area around Mauranipur and Babina lies within the Central Bundelkhand Greenstone Belt. The investigated area falls between latitude 25°09'45" N to 25°15' N, and longitude 78°25' S to 78°35' S in Babina (Fig. 3.2), as well as latitude 25°11'54" N to 25°14'48" N, and longitude 79°05' S to 79°09'35" S in Mauranipur (Fig. 3.3) of the BuC. The study area mainly covers the village of Kuraicha, the Saprar river section, and the Sukwa Dam area. The Mauranipur area lies in the centre of BuC, where the TTGs are mostly exposed and banded magnetite metavolcanic (BMM) rocks can be found locally. The terrain has a more or less subdued topography except for the ESE–WNW trending small isolated hillocks and a NE–SW trending quartz reef near Kuraicha. TTGs, ultramafic rocks, amphibolites, granitoids, pelitic granulites, garnetiferous amphibolite, quartzite, granitic

gneiss, and migmatite are the major rock types in the study area. Here, garnet-orthopyroxene pelitic granulites and garnet-biotite gneiss are exposed in the form of enclaves within TTGs. ESE–WNW trending outcrops of banded magnetite quartzite (BMQ) and quartz reefs trending NE–SW is exposed in a scattered manner. The major rock types that are uncovered in the study area are pelitic granulites, amphibolites, garnet-bearing amphibolites, high-grade gneisses, BIFs, TTGs, granitoids, and migmatitic gneiss (Singh and Dwivedi, 2015). The existence of 2–3 m thick pelitic gneiss lensoidal structures inside the TTG provides solid evidence for the assertion that high-grade metamorphism occurred before TTG emplacement in the BuC. Foliations in the gneisses have generally struck NW–SE to WNW–ESE with a steep dip ($> 70^\circ$) towards NE–NNE. Four phases of deformation, D1–D4, are identified in the area. Four deformation phases (D1–D4) have been recognized in the area. The first three stages are represented by the F1, F2, and F3 generations of mesoscopic folds, respectively, whereas the D4 deformation leads to the production of shear structures in the rocks (Singh and Dwivedi, 2015).

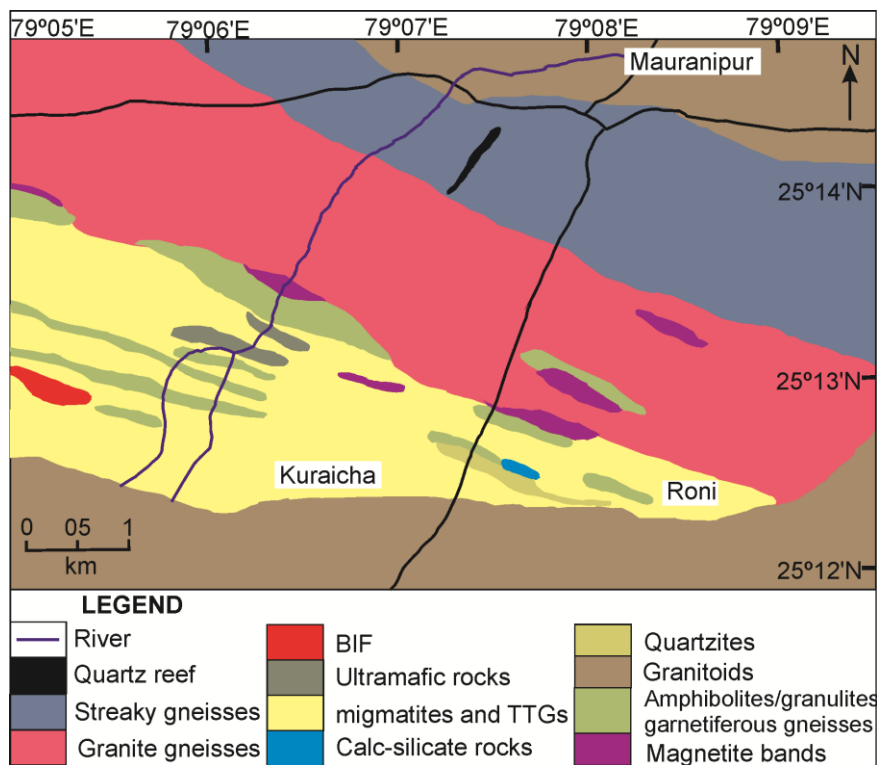


Figure 3.2 Regional geological map of the area around Mauranipur (after Singh & Dwivedi, 2015).

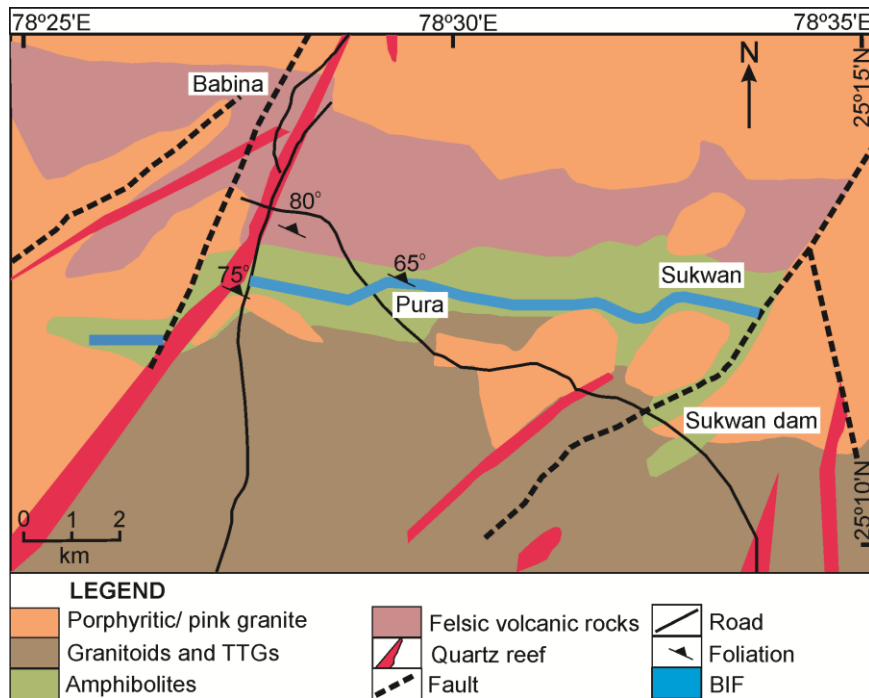


Figure 3.3 Regional geological map of the Babina and its adjacent area (after Verma et al. 2016)

3.4 Metamorphism

Several authors have discussed the metamorphic evolution of BuC (Saha et al., 2011; Nashipuri et al., 2019). The metamorphic ages described by different authors are summarized in Table 3.2. Three phases of metamorphism have been recorded in TTGs and ultramafic-mafic rocks. The metasupracrustals and felsic rocks have undergone metamorphism of amphibolites to granulite facies (Basu, 1986; Singh and Dwivedi, 2009). Amphibolite rocks found along Bundelkhand tectonic zone suggest a metamorphic event around 3.4–3.3 Ga based on Nd isotopic values (Malviya et al., 2006). Amphibolites and BIFs depict high-pressure and high-temperature metamorphism. The metamorphic age of high pressure (18–20 kbar and 630°C) metamorphism is recorded from Mg-Al white schists in the Babina area, which took place at ~ 2.78 Ga (Saha et al., 2011, Singh and Dwivedi, 2015). Based on the U-Pb and Pb-Pb ages of intrusive, felsic rocks a metamorphic event of ~2.50 Ga is marked in which large-scale granitic magmatism has occurred (Joshi et al., 2017; Singh et al., 2019). Granitoids of intrusive nature are less metamorphosed, but supracrustal rocks (amphibolites, BIFs, calc-silicate rocks, corundum bearing phengite gneiss, fuchsite quartzite, and quartzite)

show both high temperature/low pressure and high pressure/low-temperature types of metamorphism. Similarly, five distinct events of metamorphism have been reported based on SHRIMP studies in BuC between 3.20 and 0.53 Ga (Pati and Saha, 2011; Saha et al., 2016). Kaur et al. (2016) recognized a metamorphic event of Paleoproterozoic age (~3.20 Ga) in TTGs. Nashipuri et al. (2019) attempted to evaluate the structural and metamorphic history of TTGs (hornblende-plagioclase-quartz bearing assemblage) of the Babina, having metamorphism within the P - T ranges of ~6.5-8.5 kbar, 630–720°C. Low-grade metamorphism has been observed in BuC metasediments and metavolcanics with P - T conditions of 4–5 kbar and 500±50°C (Pati et al., 2020). In conclusion, four metamorphic events at ~3.30 Ga, 3.29 Ga, 3.20 Ga, ~2.78 Ga, ~2.55 Ga, ~2.48 Ga, and ~2.13 Ga have been obtained in TTGs by integrated zircon imaging and U-Pb data (Slabunov and Singh, 2019; Singh et al., 2019).

3.5 Tectonic imprint

In BuC, structural and tectonic studies have rarely been done in a few areas. TTG gneisses are present as enclaves in BuC and are characterized by three to five phases of folding (Sharma, 1982; Prasad et al., 1999; Singh et al., 2007). The foliations dip steeply (60°-70°) towards NE or SW directions. In TTGs, the most outstanding foliation is observed in melanocratic and leucocratic layers. These folded foliations developed second-stage foliations defined by biotite and hornblende. Hook-shaped folds are observed in high strain zones. The last folding phase is sinistral, producing open, steep dipping folds (Nashipuri et al., 2019). The gneisses also have sheared contacts with granites and enclaves of foliated mafic and ultramafic rocks on a centimetre to a metre scale. BIF, quartzite, calc-silicate rocks, and amphibolites show the most prominent folding. BIFs have tight-to-isoclinal F1 and F2 stage folding with sub-vertical S1 and S2 schistosity, trending E-W and parallel to F1 and F2 axial planes, respectively. The F3 folds in BIF occur as broad warps. Folds in BIFs are as crucial as they are used to calculate the shortening of the Bundelkhand basin. The "Raksa

Shear Zone" (RSZ) was a sinistral shear zone having an E-W trend and was first demarcated by [Senthappan \(1976 and 1981\)](#). The BTZ is another E-W trending tectonic zone of the Archean age having sinistral movement. It runs in the middle of BuC for hundreds of km. Because of the presence of ophiolite sequences (metamorphosed basaltic pillow lava, basaltic komatiite of boninitic affinity, metadunite, and metasediments), BTZ is thought to be of Archean age subduction zone ([Malviya et al., 2006](#)). All types of petrofabrics indicating brittle-ductile deformation (cataclastic-protomylonite-mylonite-pseudotachylites) are observed within BTZ. BTZ contains significant mineralization of BuC (iron: [Basu, 1986](#); base metal, molybdenite and gold: [Pati et al., 1997](#)).

3.6 Geochronology

BuC is of Archean age, but its various components, such as TTG gneissic complexes, extensively deformed greenstone belts, granitoids, mafic dykes, and quartz reefs, are exhumed to the surface at different times. Many scientists have tried to evaluate the age of different lithologies. The age data of BuC is summarized in [Table 3.3](#). The oldest lithology of the BuC is the TTG gneisses and is exposed in the Central and Southern greenstone belts. Zircon grains from these gneisses yield an age of 3.59–3.55 Ga ([Kaur et al., 2014](#); [Saha et al., 2016](#)). By the Rb-Sr whole rock isochron method, [Sarkar et al. \(1996\)](#) reported age of 3.5 Ga from the Baghora trondhjemitic gneiss south of Babina. TTG gneisses exposed along the Mahoba in the eastern part of the BTZ are of 3.3–3.2 Ga age ([Mondal et al., 2002](#); [Kaur et al., 2016](#); [Joshi et al., 2016](#)). Greenstone units such as mafic-ultramafic volcanic are of 3.44 Ga age, as reported by [Singh et al., 2019](#). The Sensitive High-Resolution Ion Micro Probe (SHRIMP) ages of zircon from the felsic volcanic rocks of BuC yield that they are of Neoproterozoic age and are emplaced in two episodes. One is around 2.81 Ga, and the other is around 2.6–2.54 Ga ([Mondal et al., 2002](#); [Singh and Slabunov, 2015](#)). In general, the age of granitoids decreases due south of BTZ (Bansi: 2517 ± 7 Ma; Datia: 2515 ± 5 Ma; Lalitpur:

2521 ± 5 Ma; Lalitpur leucogranite: 2492 ± 10 Ma) (Mondal et al., 2002; Pati et al., 2007; Saha et al., 2011). Mondal et al. (2002) suggest this age as the stabilization age of the craton. The mafic dykes are the youngest part of the BuC and are emplaced between 1.97 and 1.8 Ga (Sarkar, 1997). At the same time, silica-rich fluid activity filled the NNE-WSW-trending fault-bound tensile fractures in multiple phases between 1.9 and 2.1 Ga., forming giant quartz reefs. After that, the BuC continued to be tectonically active due to the large volume of pseudotachylites (>1600 Ma) that were observed dissecting granitoids and mafic dykes. Two stages of the tectonic evolution of CBGC are summarized by Singh and Slabunov (2015) and Singh et al., 2021. Amphibolites, tremolite–actinolite (high-Mg) rocks, early felsic volcanics, and chlorite biotite schist rocks are unearthed during the first stage. The early felsic volcanic rocks of the 2.8 Ga age (Meso-Archean) marked this stage. The felsic magmatic activity marks the second stage at 2.5 ± 17 Ga in the Babina greenstone belt. Both the magmatic activities are results of the subduction process, and hence, the central Bundelkhand craton was formed in a subduction–accretion setting around 2.8 Ga and 2.54 Ga.

Table 3.1 Stratigraphy with order of emplacement of different intrusives in Bundelkhand Craton (after Pati et al. 2020).

Lithological Units	Field Characters	Mineralogical Assemblages	Age (Ma/Ga)	References
Vindhyan Supergroup	Sedimentary rocks (Sandstone, Limestone etc.)	Qtz + Or ± Plag ± Bt ± Hbl	~1.6 Ga	Sarang et al., 2004
Mafic dykes	Moderate relief and highly jointed, dark greenish grey in colour, fine to medium grained with ophitic to sub-ophitic texture.	Plag ± Cpx ± Ol ± Qtz ± Ilm ± Mag	1.1-1.97 Ga	Sarkar et al., 1997; Sharma and Rahman, 2000; Rao et al., 2005; Pati et al., 2008; Pradhan et al., 2012; Radhakrishna et al., 2013.
Giant quartz veins (GQVs)	Trend: NNE-SSW to N-S. Fault breccias and subhorizontal stretching lineations preserved.	Qtz ± Sr ± Ep ± Opq ± Cal	1.9-2.2 Ga	Sarkar et al., 1984; Rao et al., 2005; Pati et al., 2007
Rhyolite/ Granophyre/ Granite Porphyry	Pinkish brown in colour, massive in nature and extensively fractured. Euhedral feldspar grains and blue quartz are present.	Qtz + Or ± Plag ± Bt ± Hbl ± Ep ± Chl	2.5±7 Ga	Mondal et al., 2002
Karera Gneiss	Enclaves within alkali granitoid gneisses.	Qtz + Plag ± Bt ± Hbl ± Ep	~2.56±6 Ga	Mondal et al., 2002; Saha et al., 2010
Intrusive Granitoids	Variations in colour, texture and mineralogy. Syenites are rare. Pegmatites are mostly anhydrous in nature.	Qtz + Or ± Plag ± Bt ± Hbl ± Ep	1.9 -2.59 Ga	Mondal et al., 2002; Pati et al., 2010; Saha et al., 2011; Kumar et al., 2013; Singh and Slabunov, 2013, 2015; Kaur et al., 2016; Verma et al., 2016; Joshi et al., 2017; Singh et al., 2019
Sanukitoids and anatectic granites	Outcrops are mostly undeformed, multiphase emplacement in all older units	Plag + Hbl ± Qtz ± Or ± Bt ± Zr ± Ap ± Aln ± Mnz ± Ttn and Qtz + Or + Plag ± Bt ± Hbl ± Zr ± Ap ± Mnz ±	2.59-2.46 Ga	Mondal et al., 2002; Pandey et al., 2011; Saha et al., 2011; Kumar et al., 2013; Kaur et al., 2016; Verma et al., 2016; Joshi et al., 2017; Singh et al., 2019

		Ttn ±Aln		
Tonalite-Trondhjemite-Granodiorite Gneisses (TTGs)	Basement unit, Enclaves within alkali granitoid gneisses. Associated with greenstone component.	Qtz + Plag ± Bt ± Hbl ± Ep	~3.6-2.7 Ga	Sarkar et al., 1995 ; Mondal et al., 2002 ; Singh and Slabunov, 2013 ; Singh and Slabunov, 2014, 2015 ; Kaur et al., 2014, 2016 ; Saha et al., 2011, 2016 ; Verma et al., 2016 ; Joshi et al., 2017 ; Singh et al., 2019 ; Nasipuri et al., 2019
Calc-silicates	Associated with amphibolites, quartzites and BIFs. At few places with karst-like topography.	Amp + Di + Qtz + K-Nafeldspar + Ap ± Cal ± Wo	—	—
Corundum-Phlogopite-Phengite Schists	Occurring within TTGs	Crn + Phl + Chl + Cln	~2.78 Ga (~age of metamorphism) ~2.47 Ga (~exhumation age)	Saha et al., 2011
Felsic volcanics	Less deformed unit, usually occur at base of BIFs and at some places, in the form of dykes	Qtz + Plag + Bt + Hbl	2.81-2.54 Ga	Slabunov et al., 2013 ; Singh and Slabunov, 2014, 2015 ; Joshi et al., 2017 ; Slabunov and Singh, 2018
Banded Iron Formations (BIFs)	Associated with metasediments, quartzites, granitoid gneisses etc. Composed of alternating layers of iron-rich and amorphous silica-rich materials. Show multiple phases of folding.	Mag + Qtz ± Opx ± Cpx ± Grt ± Hbl ± Act ± Bt ± Chl ± Ap ± Aln	2.82-2.81 Ga	Slabunov et al., 2013 ; Singh and Slabunov, 2013, 2015
Amphibolites	Mostly associated with greenstone components. At	Hbl + Plag ± Grt ± Bt ± Chl ± Qtz ± Mag ±	4.9-4.2 Ga (possibly	Malviya et al., 2005 ; Singh et al., 2019

	some places, observed as enclaves within granitoids and gneisses	Sp ± Ap ± Zr ± Mnz	protolith age) 3.4-3.3 Ga (~age of metamorphism)	
--	--	--------------------	--	--

Table 3.2 Stages of metamorphism from Paleoproterozoic to Neoproterozoic reported in different rock types in the Bundelkhand Craton

Age	Type of metamorphism	Dating Technique	Type of Rocks	Locality	Authors
M1 (3300-2700 Ma) Paleoproterozoic					
3400-3300	Medium-grade	Nd isotopic values	amphibolite	Mahoba	Malviya et al., 2005
3290	Medium-grade	Zircon	TTG gneisses	Charkhari, Mahoba	Singh et al., 2021
3270 ± 3		Zr, SIMS (²⁰⁷ Pb/ ²⁰⁶ Pb)	Gneisses, TTG	Mahoba	Mondal et al. (2002)
3249±5	Medium-grade	Zircon	Metabasic enclaves within TTG gneisses	Mahoba	Mondal et al., 2002
3220 ± 79	High-grade	Zr, LA-ICP-MS	TTG gneiss	Babina (Sukwan–Dukwan dam)	Saha et al. (2016)
3200±10	Medium-grade	Zircon	TTG gneisses	Charkhari, Mahoba	Kaur et al., 2016
3185±8	Medium-grade	Zircon	TTG gneisses	Charkhari, Mahoba	Kaur et al., 2016
3137±96	400-450 °C at 0.1-0.2 GPa	monazite	BIFs	Mauranipur	Raza et al., 2021
M2 (2700-2300 Ma) Neoproterozoic					
2780±64	Eclogite facies metamorphism (18-20kbar, 620°C-640 °C)	Zr, LA-ICP-MS	White schists	Babina	Saha et al., 2011

2730±30	High-pressure amphibolite facies metamorphism (7.2-10kbar, 580°C-680°C)	Zr, LA-ICP-MS	White schists	Babina	Saha et al., 2011
2687 ± 11	Medium-grade	Zr, SHRIMP U-Pb	metasomatic rocks	Mauranipur	Slabonov and Singh., 2019
2538±120	Prograde metamorphism	monazite	BIFs	Mauranipur	Raza et al., 2021
2500-2200	<i>P-T</i> parameters are still uncertain	zircon	White schists	Babina	Saha et al., 2011
M3 (2300-1800 Ma) Neoproterozoic					
2168±83	Retrograde metamorphism	monazite	BIFs	Mauranipur	Raza et al., 2021
1900-1800	Prehnite-pumpellyite metamorphism (3-5kbar, 150°C-250 °C)	Zircon	metavolcanics	Mauranipur	Sibelev et al., 2021
unknown	Medium pressure granulite facies	Lu-Hf	Pelitic and mafic gneisses	mauranipur	Singh and Dwivedi 2015

Table 3.3 Geochronological age data of all the rock types in the Bundelkhand Craton (after Singh et al. 2021).

Rock Types	Age(Ga/Ma)	Area	Dating Method	References	
Tonalite-Tronjhemite-Gneisses (TTGs)	2699±7.4 Ma	Babina	LA-ICP-MS	Verma et al., 2016	
	2706±11 Ma		LA-ICP-MS	Singh et al., 2021	
	2681±10 Ma		LA-ICP-MS	Singh et al., 2021	
	3440±3 Ma		LA-ICP-MS	Saha et al., 2016	
	3532±7 Ma		SHRIMP	Pati et al., 2010	
	3409±8 Ma		SHRIMP	Pati et al., 2010	
	3503±99 Ma	Mauranipur	Rb-Sr	Sarkar et al., 1996	
	3551±6 Ma		LA-ICP-MS	Kaur et al., 2014	
	3297±8 Ma		Ion-probe	Mondal et al., 2002	
	3220±79 Ma		LA-ICP-MS	Saha et al., 2016	
	3394±8.6 Ma		LA-ICP-MS	Kaur et al., 2016	
	3364±10 Ma		LA-ICP-MS	Singh et al., 2021	
	3422± 39 Ma		LA-ICP-MS	Singh et al., 2021	
	3343±85 Ma		LA-ICP-MS	Singh et al., 2021	
	3410±9 Ma		LA-ICP-MS	Singh et al., 2021	
	2712±16 Ma		LA-ICP-MS	Singh et al., 2021	
	3205±12 Ma		Girar Mahoba	LA-ICP-MS	Kaur et al., 2016
	3346±10 Ma			LA-ICP-MS	Singh et al., 2021
3280±15 Ma	LA-ICP-MS	Singh et al., 2021			
3310±2 Ma	SIMU-Pb	Joshi et al., 2017			
3285±6.7 Ma	LA-ICP-MS	Kaur et al., 2016			
3270±3 Ma	Ion probe	Slabunov et al., 2017			
Quartzite-BIF-Pelitic sediments	2733±30 Ma	Babina	Th-U-Pb EPMA	Saha et al., 2011	
	2785±49 Ma	Girar	LA-ICP-MS	Saha et al., 2011	
	3432±9.7 Ma		LA-ICP-MS	Slabunov and Singh 2019	
	3452±6.4 Ma		LA-ICP-MS	Slabunov and Singh 2019	
	3290 Ma		Nd Modal age	Slabnuov et al., 2017	
Granodioritic gneisses	2358±46 Ma	Babina	LA-ICP-MS	Kaur et al., 2016	
	2561±11 Ma	Karera	LA-ICP-MS	Kaur et al., 2016	

	2546±6 Ma 2551±7 Ma 2566±11 Ma	Lalitpur Jhansi Mahoba	LA-ICP-MS LA-ICP-MS LA-ICP-MS	Kaur et al., 2016 Kaur et al., 2016 Kaur et al., 2016
Mafic-Ultramafic volcanics	3440±163 Ma 4.9-3.3 Ga 2687±11 Ma 4.5-3.4 Ga 3249±5 Ma 4.2-3.4 Ga	Babina Mauranipur Mahoba	Sm-Nd isochron SHRIMP Nd Modal age Ion probe Nd Modal age	Singh et al., 2019a Malviya et al., 2005 Slabunov and Singh 2019 Malviya et al., 2005 Mondal et al., 2002 Malviya et al., 2005
Felsic volcanics-Dacite-Rhyolite	2542±17 Ma 3140 Ma 2517±7 Ma 2557±33 Ma 2810±13 Ma	Babina Bansi Mauranipur	SHRIMP Nd Modal age Ion probe SHRIMP SHRIMP	Singh and Slabunov 2015 Singh and Slabunov 2015 Mondal et al., 2002 Slabunov and Singh 2019 Slabunov and Singh 2019
K-rich granitoids	2556±23 Ma 2557±16 Ma 2546±3 Ma 2516±38 Ma 2514±13 Ma 2525±25 Ma 2554±3 Ma 2539±7 Ma 2563±6 Ma 2583±10 Ma 2563±11 Ma 2554±5 Ma 2564±42 Ma 2521±7 Ma 2592±10 Ma 2578±22 Ma 2545±10 Ma 2548±8 Ma	Babina Bansi Karera Lalitpur Mauranipur	LA-ICP-MS LA-ICP-MS SIMU-Pb LA-ICP-MS LA-ICP-MS LA-ICP-MS SIMU-Pb LA-ICP-MS Ion probe LA-ICP-MS LA-ICP-MS LA-ICP-MS LA-ICP-MS Ion probe Ion probe SIMU –Pb LA-ICP-MS LA-ICP-MS	Singh et al., 2021 Singh et al., 2021 Joshi et al., 2017 Verma et al., 2016 Kaur et al., 2016 Kaur et al., 2016 Joshi et al., 2017 Kaur et al., 2016 Mondal et al., 2002 Kaur et al., 2016 Kaur et al., 2016 Kaur et al., 2016 Kaur et al., 2016 Kaur et al., 2016 Mondal et al., 2002 Mondal et al., 2002 Joshi et al., 2017 Kaur et al., 2016 Kaur et al., 2016

	2553±6 Ma 2563±7 Ma 2560±7 Ma 2557±19 Ma 2569±19 Ma 2562±6 Ma 2531±21 Ma 2529±8 Ma 2566±14 Ma 2537±8 Ma 2515±5 Ma 2549±13 Ma 2482±7 Ma 2565±8 Ma 2561±35 Ma 2491±17 Ma	Dhala Jhansi Mahoba Khajuraho Tikamgarh	SHRIMP SHRIMP SIMU-Pb SIMU-Pb SIMU-Pb SIMU-Pb LA-ICP-MS LA-ICP-MS LA-ICP-MS LA-ICP-MS Ion probe LA-ICP-MS Ion probe SIMU-Pb LA-ICP-MS LA-ICP-MS	Pati et al., 2010 Pati et al., 2010 Joshi et al., 2017 Joshi et al., 2017 Joshi et al., 2017 Joshi et al., 2017 Kaur et al., 2016 Kaur et al., 2016 Kaur et al., 2016 Kaur et al., 2016 Mondal et al., 2002 Kaur et al., 2016 Mondal et al., 2002 Joshi et al., 2017 Kaur et al., 2016 Kaur et al., 2016
Sanuktoids	2566±2 Ma 2559±7 Ma 2568±12 Ma 2544±6 Ma	Karera Jhansi Khajuraho	SIMU-Pb SIMU-Pb LA-ICP-MS SIMU-Pb	Joshi et al., 2017 Joshi et al., 2017 Singh et al., 2021 Joshi et al., 2017
Quartz reef	1866±11 Ma 1779±43 Ma	Babina	SHRIMP SHRIMP	Slabunov et al., 2017